NUCL SCI TECH (2017) 28:183
https://doi.org/10.1007/s41365-017-0331-7

Identifying defect energy levels using DLTS under different electron irradiation conditions

Chun-Sheng Guo[1,2,3] · Ruo-Min Wang[1] · Yu-Wei Zhang[2] · Guo-Xi Pei[3] · Shi-Wei Feng[1] · Zhao-Xian Li[2]

Received: 1 November 2016 / Revised: 23 February 2017 / Accepted: 2 March 2017 / Published online: 28 November 2017

Abstract Electron beams of 0.5, 1.5, 2.0, and 5.0 MeV were used to irradiate n-Si diodes to fluences of 5.5×10^{13}, 1.7×10^{14}, and 3.3×10^{14} e cm^{-2}. The forward voltage drop, minority carrier lifetime, and deep level transient spectroscopy (DLTS) characteristics of silicon p–n junction diodes before and after irradiation were compared. At the fluence of 3.3×10^{14} e cm^{-2}, the forward voltage drop increased from 1.25 V at 0.5 MeV to 7.96 V at 5.0 MeV, while the minority carrier lifetime decreased significantly from 7.09 μs at 0.5 MeV to 0.06 μs at 5.0 MeV. Six types of changes in the energy levels in DLTS spectra were analyzed and discussed.

Keywords Electron irradiation · Deep level transient spectroscopy (DLTS) · Minority carrier life time · Silicon diode

1 Introduction

Irradiation is a primary way of controlling the carrier lifetime in p–n junctions. It has been shown that irradiation creates defect energy levels (which act as recombination centers in semiconductor materials), reduces the minority carrier lifetime, and increases the switching speed [1, 2]. Electron beams (EB) were used to irradiate crystalline silicon or silicon devices to different irradiation fluences, and the defect energy levels or the device performances before and after irradiation were analyzed [3–7]. The effects of EB energy and the effects of combined EB and γ-ray irradiations were studied, too [8, 9], with different parameter values in the carrier number, location, and concentration of the defect energy levels. Using 2 MeV EB to irradiate crystalline n-Si manufactured by applying the Czochralski method (Cz) and the Floating Zone method (Fz), Takakura et al. [10] found four defect energy levels in Cz-Si (E_c—0.39, E_c—0.26, E_c—0.18, and E_c—0.09 eV) and three defect levels in Fz-Si (E_c—0.59, E_c—0.40, and E_c—0.23 eV). Zangenberg et al. [11] found seven defect levels by irradiating a p-Si diode at 20–40 K using 2 MeV EB. Kang et al. [12] used 12 MeV EB to irradiate a p-Si p–n junction diode and found two defect levels at E_c—0.284 and E_c—0.483 eV. Cai et al. [13] and Ma et al. [14] found four defect levels using 1.5 MeV EB to irradiate n-Si wafer produced with the Czochralski method.

In this work, n-Si rectifier diodes were irradiated to fluence of 5.5×10^{13}, 1.7×10^{14}, and 3.3×10^{14} e cm^{-2} by electron beam of 0.5, 1.5, 2.0, and 5.0 MeV. Their forward voltage drop, minority carrier lifetime, and the deep level transient spectroscopy (DLTS) characteristics were measured before and after irradiation. Based on the measurements, the irradiation effects on the defect energy levels were analyzed. The observations included appearance and disappearance of the energy levels, changes in the defect concentration, and positional shift of the energy levels.

This work was supported by the Beijing education and scientific research department (No. KM201510005008).

✉ Chun-Sheng Guo
guocs@bjut.edu.cn

1 College of Electronic Information and Control Engineering, Beijing University of Technology, Beijing 100124, China

2 Wuxi EL Pont Group, Wuxi 214151, China

3 Institute of High Energy Physics, Chinese Academy of Sciences, Beijing 100049, China

2 Experimental

The samples were 1A/1000V rectifier diodes, type 1N4007, packaged in DO-41 plastic, and manufactured by MIC. They were fabricated using a triple-diffusion process on a Cz ⟨111⟩-oriented 60-Ω cm N-type silicon substrate. The doping element was phosphorus (7×10^{13} cm^{-3}) in the n region and boron (1.8×10^{19} cm^{-3}) in the p regions. The chip was 230 μm thick, packaged in a cylinder of Φ2.7 mm × 5.2 mm. The samples were divided into 13 groups, each containing three diodes. Twelve groups were irradiated, respectively, by 0.5, 1.5, 2.0, and 5.0 MeV EB to fluences (Φ_n) of 5.5×10^{13}, 1.7×10^{14}, and 3.3×10^{14} e cm^{-2}. The control was not irradiated. Before and after irradiation, the forward voltage drop (V_F) was tested using a semiconductor device parameter analyzer (Agilent Technologies B1500A), with a forward current of 1 A. The minority carrier lifetime (τ) and DLTS characteristics were measured using an instrument made by Nanjing University. All the irradiated samples were tested under ambient temperatures and pressures, after stored at room temperature for 120 h so as to avoid the annealing effect owing to the instability of the defects under irradiation [15].

The irradiations were carried out on a linear electron accelerator of the Wuxi EL Pont Group, with electron beams of 0.1 mA in current instability $< \pm 2\%$ and non-uniformity $< \pm 5\%$. During the irradiation, the sample temperature remained blow 323 K ensured by the wind and water cooling systems, so as to minimize the EB annealing effect.

3 Results and discussion

3.1 Changes in forward voltage drop

The defect energy levels introduced by electron irradiation in semiconductor materials affect electrical properties of a device. The forward voltage drop of the samples was measured, and the results are shown in Fig. 1. The V_F of the irradiated samples increased with the irradiation fluence and the EB energy, indicating the beam energy effects.

3.2 Changes in minority carrier lifetime

The exact locations and concentrations of deep energy levels in a semiconductor have a significant impact on minority carrier lifetime of the device. To ensure that the concentration of the deep level defects introduced by EB irradiation is sufficient to carry out DLTS measurements, we measured the minority carrier lifetime of the devices.

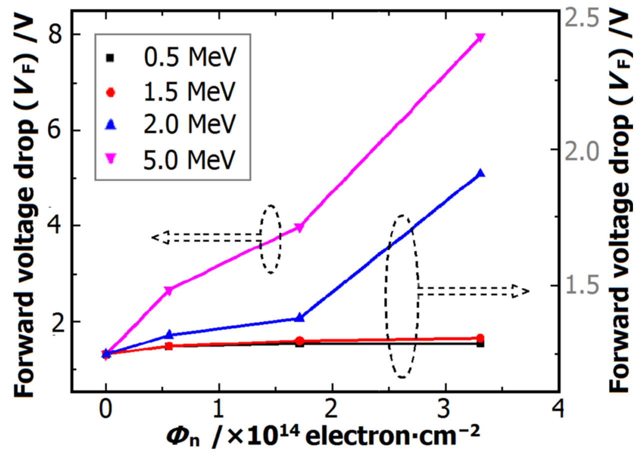

Fig. 1 (Color online) Forward voltage drop V_F as z function of the irradiation fluence Φ_n, at electron beam energies of 0.5–5.0 MeV

Figure 2 shows the minority carrier lifetime of the devices irradiated under different EB energies, as a function of the irradiation fluence. The experimental data were averaged for each group. The results show that at 0.5 MeV, the minority carrier lifetime changed little, while it was reported that 0.5 MeV was a lattice atom displacement threshold [16]. This may be because that the diode packaging in this work was thicker, or the electron beam density in this work was lower. At 1.5, 2.0, and 5.0 MeV, the minority carrier lifetime decreased with increasing fluences, and the amplitude increased with EB energy. We calculated the reciprocal of the minority carrier lifetime. As shown in Fig. 2b, the τ^{-1} has a good linear relationship with the irradiation fluence Φ_n. For radiation damage in semiconductors, according Ref. [1], the minority carrier lifetime is related to irradiation fluence by $1/\tau = 1/\tau_0 + k\Phi_n$, where τ_0 and τ are the minority carrier lifetime before and after irradiation, respectively; k is the irradiation damage coefficient; and Φ_n is the irradiation fluence. From the slopes in Fig. 2b, we have $k = (4.78 \pm 1.24) \times 10^{-16}$ at 1.5 MeV, $(5.06 \pm 0.96) \times 10^{-15}$ at 2.0 MeV, and $(4.96 \pm 0.40) \times 10^{-14}$ at 5.0 MeV, i.e., the degradation rate of minority carriers increases with the beam energy.

3.3 Changes in defect energy levels

The principle and formula of DLTS analysis in Refs. [17, 18] were used. We used the rate window method, using liquid nitrogen to complete a slow temperature scan from low to high temperatures. During this period, the sample was held under an appropriate reverse bias voltage of 15 V, and then a periodic forward pulse of 1 V was superimposed on the bias to check the capacitance in a fixed time interval. The rate window was $t_2/t_1 = 2$, and the control did not show deep energy levels. Because the minority carrier lifetime changes were the most significant

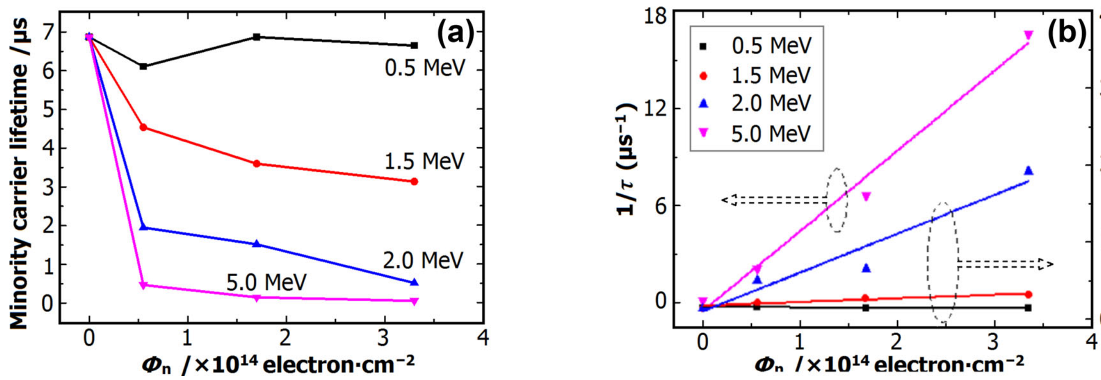

Fig. 2 (Color online) Minority carrier lifetime τ versus irradiation fluence Φ_n (**a**) at different EB energies, and the fitting curves (**b**) of Φ_n and τ^{-1}

at 2.0 or 5.0 MeV, we chose the two sets of samples for the DLTS measurements. The results are shown in Fig. 3.

The characteristics of the DLTS include the energy level position E_T relative to the conduction or valence energy level (i.e., E_c–E_T or E_T–E_v), the energy level concentration N_T, and the capture cross section σ_T. The higher is the spectral peak, the greater is the energy level concentration; the larger the X axis value is, the deeper is the energy level. While a spectral peak is a minority carrier trap, a valley-like spectral peak is a majority carrier trap. The detailed information about the relationship between DLTS spectra and irradiated defects can be found in Refs. [16, 19].

In n-Si, the majority carrier defects trap electrons, while the minority carrier defects trap holes. The filling and emission process of electrons and holes in the defect energy levels can cause changes in the junction capacitance, which yield the DLTS signal. The majority carrier level can also be observed in the minority carrier energy spectrum. However, measuring the majority carrier level in such a way does not yield accurate results because of the compensation between majority and minority carrier levels. Therefore, a separate measurement was conducted to measure the majority carrier level spectrum.

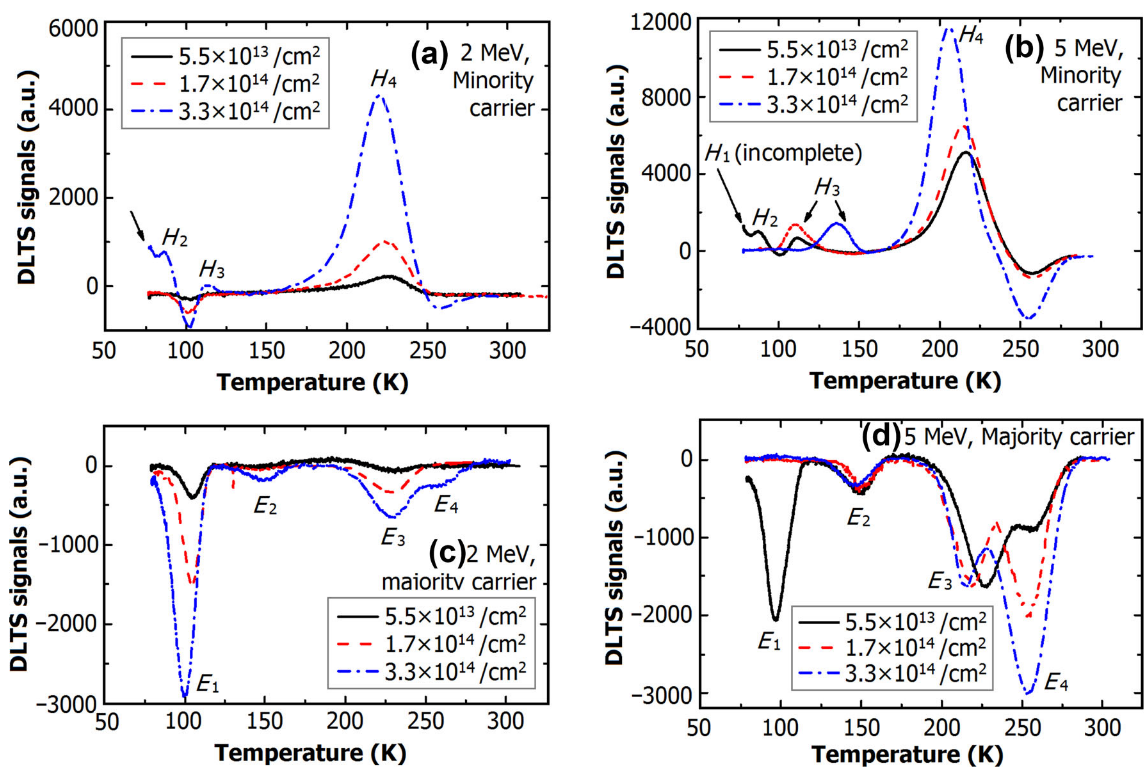

Fig. 3 (Color online) Deep level transient spectroscopy of the minority and minority carriers from the samples irradiated by 2.0 and 5.0 MeV electron beams

In Fig. 3, at 2.0 MeV and $\Phi_n = 3.3 \times 10^{14}$ cm^{-2}, and at 5.0 MeV and $\Phi_n = 5.5 \times 10^{13}$ cm^{-2}, the spectra had four minority carrier defect energy levels (H_1–H_4) and four majority carrier defect energy levels (E_1–E_4). The number of energy levels differed with the other irradiation conditions. The specific parameters of each energy level are shown in Table 1. Among the parameters, the position of the energy levels H_1–H_4 is expressed as E_T–E_v, while E_1–E_4 are expressed as E_c–E_T (where E_c is the conduction band energy, E_v is the valence band energy, and E_T is the measured energy level); N_T denotes the energy level concentration (i.e., the concentration of lattice defects). The possible formation reason and characteristics of the defect levels were discovered by comparing our results with those in Refs. [16, 20]. Not all parameters for H_1 are given in Table 1 as the sample-cooling liquid nitrogen is 77 K.

The results show that the defect energy levels introduced by electron irradiation may decrease, disappear, and move under certain conditions, in addition to appearing when the energy and fluence reaches a certain threshold and increasing with the fluence. The changes in each energy level can be categorized in six ways as follows:

(1) Appearance of spectral peaks. At 2.0 MeV and 3.3×10^{14} cm^{-2}, the energy levels H_1, H_2, H_3, E_2, and E_4 appeared. This demonstrates that during the irradiation, some defect energy levels require this fluence threshold value in addition to the energy

Table 1 Deep level transient spectroscopy spectral level parameters

DLTS peak identity	EB energy (MeV)	EB fluence (10^{14} cm^{-2})	Position E_T–E_v (eV) E_c–E_T (eV)	Concentration N_T (10^{12} cm^{-3})	Capture cross section σ_T (10^{-17} cm^2)
H_2	2.0	3.3	0.142	2.10	3800
V-related	5.0	0.55	0.148	3.43	1700
H_3	2.0	3.3	0.157	1.75	150
H-related	5.0	0.55	0.155	1.82	180
(C_iO_i–H)		1.7	0.152	3.71	150
		3.3	0.187	3.92	95
H_4	2.0	0.55	0.355	0.63	280
C_i–O_i		1.7	0.333	2.03	97
		3.3	0.315	7.70	54
	5.0	0.55	0.287	13.40	26
		1.7	0.274	17.30	11
		3.3	0.241	29.80	3.2
E_1	2.0	0.55	0.158	0.77	280
$VO^{-/0}$ (C_iC_s)		1.7	0.163	2.59	600
		3.3	0.148	5.18	250
	5.0	0.55	0.136	5.53	120
E_2	2.0	3.3	0.168	0.35	1.6
$V_2^{2-/-}$	5.0	0.55	0.162	1.19	1.0
		1.7	0.168	1.05^2	26
		3.3	0.213	0.91	78
E_3	2.0	0.55	0.350	0.21	57
VO-H		1.7	0.350	0.63	70
		3.3	0.344	1.12	48
	5.0	0.55	0.345	4.41	62
		1.7	0.308	4.41	2.8
		3.3	0.283	4.41	6.4
E_4	2.0	3.3	0.378	0.49	23
$V_2^{-/0}$	5.0	0.55	0.426	2.45	280
		1.7	0.419	6.02	220
		3.3	0.413	8.12	170

already required to achieve the material displacement threshold [21].

(2) Disappearance of spectral peaks. At 5.0 MeV and 5.5×10^{13} cm^{-2}, the energy levels H_1, H_2, and E_1 appeared. This is possibly because that the EB energy and fluence reached the highest threshold value of the samples, and the semiconductor materials were compensated especially at low temperatures. The concentration of deep defect energy levels is too high, so that free electrons and holes jump to the energy levels the closest to the mid-gap at low temperatures, such as H_4, E_3, and E_4. This leads to very low number of free electrons and holes in the conduction and valence energy levels, and thus the filling and firing processes cannot be completed in the shallow energy levels, preventing them from being scanned using DLTS, and the spectra are distorted at low temperatures.

(3) Increase in peak height. The energy levels H_4, E_1, and E_3 at 2.0 MeV, and the energy levels H_4 and E_4 at 5.0 MeV, increased with the fluence (e.g., the H_4 level concentration increased from 6.30×10^{11} to 7.70×10^{12} cm^{-3} at 2.0 MeV, and from 1.34×10^{13} to 2.98×10^{13} cm^{-3} at 5.0 MeV). With the increased total number of electrons injected into the semiconductor per unit time, the collision probability and frequency of the incident electrons with the lattice atoms increased, resulting in the increase in defect concentration.

(4) Decrease in peak value. At 5.0 MeV, the peak height of energy level E_2 decreased slightly (from 1.19×10^{12} to 9.10×10^{11} cm^{-3}). Possibly, this is because that the radiation-induced defects were unstable and were prone to annealing effects as the temperature increased. Although the environmental heat dissipation was increased, lattice atom vibrations caused by energy exchange between the electrons and lattice atoms were still intense. Therefore, the EB irradiation process can be regarded as a short annealing process in the crystal lattice [22], resulting in a decreased concentration of unstable defects. Also, the same as the disappearance of spectral peaks, another reason may be the excessive radiation caused spectral distortion at low temperatures.

(5) Little change in peak value. At 5.0 MeV, the height of energy level E_3 changed little. This shows that some energy levels reached concentration saturation under certain irradiation conditions and no longer increased with the fluence.

(6) Peak position shift. At 2.0 MeV, energy levels H_4 and E_1 shifted to the left. (The energy level became shallower.) At 5.0 MeV, energy levels H_4, E_2, E_3, and E_4 shifted to the left, but energy level H_3 shifted right finally. (The level became deeper.)

In the DLTS spectra, different types of energy levels can compensate each other. When that happens, the minority and majority carrier peaks appear at the same or at a similar position. Two peaks mutually compensating each other leads to a visible peak reduction. The same type of energy levels can be superimposed on each other. If several minority or majority carrier peaks appear at the same or at similar positions, they will overlap and form a new peak. The left-shifting of peak position as the fluence increases may have two explanations:

(1) The energy levels are each composed of a few energy levels that are close in position: as the concentration of the shallower energy levels increases, the position of entire energy level shifts left.

(2) Owing to the increase in the concentration of defect energy levels, the trapping ability is enhanced for both electrons and holes. The filling and emission processes of the electrons and holes in the energy level will occur at lower temperatures, resulting in the left-shift of energy level.

At 5.0 MeV, the peak of energy level H_3 shifted left first and then right. This may be due to a new energy level emerged at a deeper position at 3.3×10^{14} cm^{-2}. The new energy level and the original level H_3 superimposed on each other, resulting in the position shift.

The concentrations of defect levels change with the irradiation conditions, while the compensation and superposition effects between different energy levels change the positions of the peak, e.g., the position of energy level H_4 ranged from E_c—0.355 to E_c—0.241 eV (a difference of 0.114 eV). This may be one of the reasons why the energy level positions always fluctuated within a certain range in previous studies.

In EB irradiation of semiconductors, the electrons enter the lattice and impact the lattice atoms, leaving the original positions of the atoms to enter the gap. Vacancy and interstitial atoms will be formed, i.e., the Frenkel defects. These defects can form more complex defects with impurities in the semiconductors, such as oxygen vacancy pairs, phosphorus vacancy pairs, and double vacancy pairs. If the energy levels of the defects lie within the forbidden band, they will act as a compound center, compounding carriers. To visualize the position of each energy level clearly, we used band diagrams. As an example, the band diagram for a 2.0 MeV electron beam with a fluence of 3.3×10^{14} e cm^{-2} is shown in Fig. 4.

The majority carrier levels E_1–E_4 positions (E_c–E_T) are acceptor levels, which capture electrons, while the minority

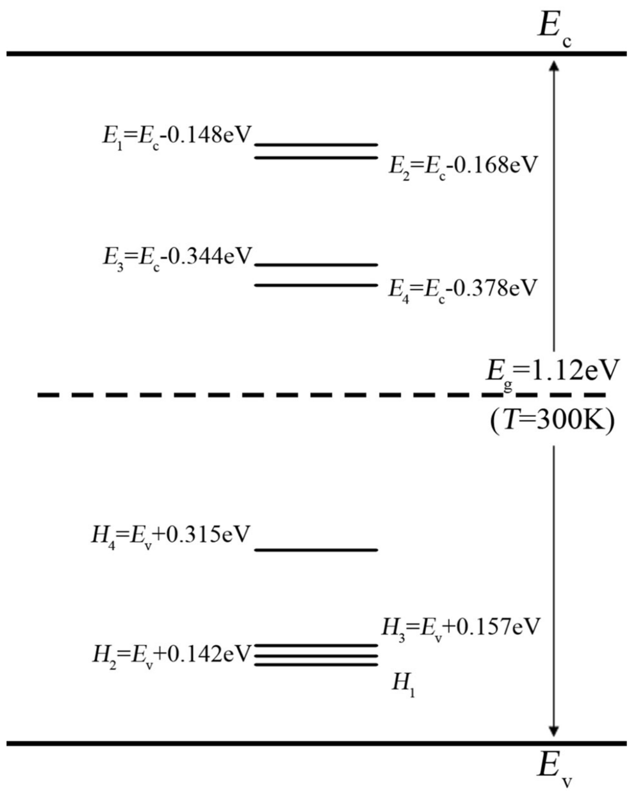

Fig. 4 Energy band diagram at 2.0 MeV and 3.3 × 10^{14} cm^{-2}

carrier levels H_1–H_4 (E_T–E_v) are donor levels, which capture holes. The efficiency of lifetime control is related to the position, concentration, and capture cross section of the defect energy levels. The effect of defect energy levels near the mid-gap on carrier recombination is more obvious than that of the shallow levels. In this work, the E_3, E_4, and H_4 levels were located closest to the mid-gap, and their concentrations were much higher, so these defect energy levels caused a rapid decrease in the minority carrier lifetime. This is consistent with our results on the minority carrier lifetime.

4 Conclusion

This paper studied the effects of different electron irradiation conditions on the various characteristics of the defect energy levels of n-Si diodes. This result should provide a useful reference for future studies on the use of irradiation for improving the performances of materials or the lifetime control technique.

(1) When the irradiation energy exceeded the threshold value (1.5 MeV, in this paper), defect energy levels could be introduced into a package diode in the form of composite centers via electronic radiation. In addition, greater irradiation energies led to higher radiation damage factors k and faster reductions of the minority carrier lifetimes.

(2) For irradiation energies of 2.0 and 5.0 MeV, the DLTS measurement results found that under certain conditions the samples displayed a maximum of four minority carrier defect energy levels (H_1–H_4) and four majority carrier defect levels (E_1–E_4). The energy level positions, relative concentrations, and capture cross sections were calculated.

(3) The reason behind why the position and concentration of the defect energy levels changed under different irradiation conditions was determined. The data analysis included spectral peaks to appear and disappear; the increase, decrease, or lack of change of the peak values; and peak position shifts.

References

1. R.O. Carlson, Y.S. Sun, H.B. Assalit, Lifetime control in silicon power devices by electron or gamma irradiation. IEEE Trans. Electron Devices **24**, 1103–1108 (1977). https://doi.org/10.1109/T-ED.1977.18884
2. B.J. Baliga, E. Sun, Comparison of gold, platinum, and electron irradiation for controlling lifetime in power rectifiers. IEEE Trans. Electron Devices **24**, 685–688 (1977). https://doi.org/10.1109/T-ED.1977.18803
3. C. Codreanu, E. Iliescu, V. Obreja, Silicon diode electrical characteristics under electron-beam irradiation conditions-experiments and theoretical interpretation, in *IEEE semiconductor conference CAS 2001 proceedings international*, vol. 2001, pp. 481–484 (2001). https://doi.org/10.1109/SMICND.2001.967510
4. L. Pína, J. Vobecký, High-power silicon P–i–N diode with cathode shorts: the impact of electron irradiation. Microelectron. Reliab. **53**, 681–686 (2013). https://doi.org/10.1016/j.microrel.2013.02.008
5. S. Krishnan, G. Sanjeev, M. Pattabi, Electron irradiation effects on the Schottky diode characteristics of p-Si. Nucl. Instrum. Methods Phys. Res. **266**, 621–624 (2008). https://doi.org/10.1016/j.nimb.2007.11.049
6. J. Vobecký, P. Hazdra, V. Záhlava, Impact of the electron, proton and helium irradiation on the forward *I*–*V*, characteristics of high-power P–i–N diode. Microelectron. Reliab. **43**, 537–544 (2003). https://doi.org/10.1016/S0026-2714(03)00023-4
7. B. Zhao, Y. Jia, Y. Wu et al., Influence of platinum diffusion electron irradiation on performance of FRDs. Semicond. Technol. **2016**, 37–41 (2016). https://doi.org/10.13290/j.cnki.bdtjs.2016.01.007
8. U.L. Dong, E.K. Kim, B.C. Lee et al., Characterization of electron irradiated GaN n^+-p diode. Thin Solid Films **516**, 3482–3485 (2008). https://doi.org/10.1016/j.tsf.2007.08.050
9. H. Ohyama, T. Hirao, E. Simoen et al., Impact of lattice defects on the performance degradation of Si photodiodes by high-temperature gamma and electron irradiation. Physica B **308**, 1226–1229 (2001). https://doi.org/10.1016/S0921-4526(01)00949-8
10. K. Takakura, H. Ohyama, T. Yoshida et al., Comparison of electron irradiation effect on thermal donors in Cz and oxygen

doped Fz silicon. Physica B **340**, 1022–1025 (2003). https://doi.org/10.1016/j.physb.2003.09.115
11. N. Zangenberg, J.J. Goubet, A.N. Larsen, On-line DLTS investigations of the mono- and di-vacancy in *p*-type silicon after low temperature electron irradiation. Nucl. Instrum. Methods Phys. Res. **186**, 71–77 (2002). https://doi.org/10.1016/S0168-583X(01)00876-X
12. S.M. Kang, T.J. Eom, S.J. Kim et al., Reverse recovery characteristics and defect distribution in an electron-irradiated silicon *p*–*n* junction diode. Mater. Chem. Phys. **84**, 187–191 (2004). https://doi.org/10.1016/j.matchemphys.2003.11.030
13. L.L. Cai, *Investigation of the Effect of Electron Irradiated Defects in Czochralski Silicon*. M.S. Thesis, Hebei University of Technology (2007)
14. X.W. Ma, *Effect of Electron Irradiation on the Properties of Monocrystalline Silicon*. M.S. Thesis, Hebei University of Technology (2010)
15. M. Lv, X.L. Zhang, Y.X. Zhang et al., Ionizing irradiation effects for emitter perimeter area ratios of the bipolar transistor. Semicond. Technol. **2013**, 222–226 (2013). https://doi.org/10.3969/j.issn.1003-353x.2013.03.013
16. P. Hazdra, J. Vobecký, H. Dorschner et al., Axial lifetime control in silicon power diodes by irradiation with protons, alphas, low- and high-energy electrons. Microelectron. J. **35**, 249–257 (2004). https://doi.org/10.1016/S0026-2692(03)00194-0
17. D.V. Lang, Fast capacitance transient appartus: application to ZnO and O centers in GaP *p*–*n* junctions. J. Appl. Phys. **45**, 3014–3022 (1974). https://doi.org/10.1063/1.1663718
18. M. Schulz, N.M. Johnson, Evidence for multiphonon emission from interface states in MOS structures. Solid State Commun. **25**, 481–484 (1978). https://doi.org/10.1016/0038-1098(78)90162-X
19. K.L. Wang, A determination of interface state energy during the capture of electrons and holes using DLTS. IEEE Trans. Electron Devices **26**, 819–821 (1979). https://doi.org/10.1109/T-ED.1979.19503
20. G.D. Watkins, J.W. Corbett, Defects in irradiated silicon: electron paramagnetic resonance of the divacancy. Phys. Rev. **138**, 543–555 (1965). https://doi.org/10.1103/PhysRev.138.A543
21. Ö. Güllü, Ş. Aydoğan, K. Şerifoğlu et al., Electron irradiation effects on the organic-on-inorganic silicon Schottky structure. Nucl. Instrum. Methods Phys. Res. **593**, 544–549 (2008). https://doi.org/10.1016/j.nima.2008.05.043
22. Z.L. Chen, W. Yue, Z.L. Li et al., Improvement on reverse breakdown characteristics of the bipolar switching transistor by the electron irradiation. Semicond. Technol. **2014**, 943–946 (2014). https://doi.org/10.13290/j.cnki.bdtjs.2014.12.012